Vol 14 No 10, October 2005
1009-1963/2005/14(10)/2127-06

Chinese Physics

© 2005 Chin. Phys. Soc.
and IOP Publishing Ltd

Crystal field analysis of the magnetic properties of RFe$_{11}$Ti and RFe$_{11}$TiH (R=Sm, Tb, Ho)*

Su Gang(宿 刚)[a], Yan Yu(闫 羽)[a,b]†, Xu Shu-Wei(许淑伟)[a],
Du Xiao-Bo(杜晓波)[a], Jin Han-Min(金汉民)[a], and Wang Xiang-Qun(王向群)[a]

[a] *Department of Physics, Jilin University, Changchun 130023, China*

[b] *State Key Laboratory for Superhard Materials, Jilin University, Changchun 130012, China*

(Received 18 March 2005; revised manuscript received 11 May 2005)

The crystalline-electric-field parameters A_{nm} for RFe$_{11}$Ti and RFe$_{11}$TiH (R=Sm, Tb, Ho) are evaluated by fitting calculations to the magnetization curves measured on the single crystals or on magnetically aligned powder samples at 4.2K and higher temperatures. Interstitial hydrogen atom in RFe$_{11}$Ti has been found to have a significant effect on crystalline-electric-field parameters A_{nm}. By using the parameters of exchange field $2\mu_{\rm B}H_{\rm ex}$ estimated from inelastic neutron scattering experiments and the fitted A_{nm}, the calculations can reproduce the experimental curves well.

Keywords: magnetization curves, magnetic anisotropy, rare-earth compounds, Crystalline-electric-field

PACC: 7560E, 7530G, 7550B, 7510D

1. Introduction

The magnetic properties of RFe$_{11}$Ti and their hydrides RFe$_{11}$TiH have attracted much attention in the last decades.[1−14] The insertion of interstitial hydrogen element into RFe$_{11}$Ti results in an apparent change of their magnetic properties (Curie temperature, saturation magnetization and magneto-crystalline anisotropy). The magnetization measurements for RnFe$_{11}$Ti and RnFe$_{11}$TiH (Rn: Y, Lu) single crystals show that interstitial H atom in RFe$_{11}$Ti slightly enhances the uniaxial anisotropy and the magnetization of Fe-sublattice.[3,4,15] It is known that the magneto-crystalline anisotropy (MCA) of rare-earth R ion in the R-Fe inter-metallic compounds originates from the crystalline-electric-field (CEF) interaction and the values of CEF parameters are usually obtained by fitting the magnetization curves for the single crystal or the magnetically aligned powder sample.[16,17] Nikitin *et al* evaluated the values of Ho-Fe exchange field $2\mu_{\rm B}H_{\rm ex}$ and CEF parameters A_{nm} in HoFe$_{11}$TiH$_x$ (x=0,1) by fitting calculations to the magnetization curves along the crystal axis at 4.2K and concluded that hydrogenation led to an about 10% increase in $2\mu_{\rm B}H_{\rm ex}$.[1] Inelastic neutron scattering (INS) experiments on RFe$_{11}$Ti and RFe$_{11}$TiN (R=Gd, Er) show that the insertion of N element leads to a ∼14% decrease in $2\mu_{\rm B}H_{\rm ex}$.[12] The INS experiments on Gd$_2$Fe$_{17}$ and Gd$_2$Fe$_{17}M_x$ (M: C, N and D (deuterium)) also show that the insertion of the light interstitial elements decreases the Gd–Fe exchange field on the Gd ion.[18] In this connection, the insertion of light interstitial elements in R-Fe compounds causes an increase in the cell volume and inter-atomic distances of the compounds. This increase may reduce the hybridization/exchange interaction between the Fe 3d and rare earth 5d electrons, which accompanies the reduction in indirect coupling between the Fe 3d and rare earth 4f electrons according to the idea that the couplings are mediated via 5d conduction electrons.

This work is to evaluate the CEF parameters A_{nm} of RFe$_{11}$Ti and RFe$_{11}$TiH (R=Sm, Tb, Ho) from the experimental magnetization curves at 4.2K and higher temperatures based on the single-ion model and analyses of the experimental data.

2. Method of analysis

*Project supported by the Department of Science and Technology of Jilin Province, Specialized Research Fund for the Doctoral Program of Higher Education and the National Natural Science Foundation of China (Grant No 10304006).

†Corresponding author, E-mail: yanyu@mail.jlu.edu.cn

$R\mathrm{Fe}_{11}\mathrm{TiH}_x$ (x=0, 1) have a ThMn_{12}-type tetragonal structure with space group $I4/mmm$. There is one rare-earth ion site with the point symmetry D_{4h}. The Hamiltonian of the rare-earth ion consists of the spin-orbital coupling interaction, the CEF interaction, the R-Fe exchange interaction and the Zeeman energy, i.e.

$$H = \lambda \boldsymbol{L}\cdot\boldsymbol{S} + H_{\mathrm{CEF}} + 2\mu_{\mathrm{B}}\boldsymbol{S}\bullet\boldsymbol{H}_{\mathrm{ex}} + \mu_{\mathrm{B}}(\boldsymbol{L}+2\boldsymbol{S})\bullet\boldsymbol{H}. \quad (1)$$

In the coordinate system with the x' and z' axes along the [100] and [001] axes, respectively, the CEF interaction can be expressed as

$$H_{\mathrm{CEF}} = \sum_{n=2,4,6} A_{n0}\sum_j C_{n0}(\theta_j,\varphi_j) + \sum_{n=4,6} A_{n4}\sum_j (C_{n4}(\theta_j,\varphi_j) + C_{n-4}(\theta_j,\varphi_j)), \quad (2)$$

where

$$C_{nm}(\theta_j,\varphi_j) = [4\pi/(2n+1)]^{1/2} Y_{nm}(\theta_j,\varphi_j), \quad (3)$$

$Y_{nm}(\theta_j,\varphi_j)$ are the spherical harmonics, θ_j and φ_j are the polar and azimuthal angles of the position vector of jth 4f electron. It is assumed that the rare-earth ion is trivalent and $\boldsymbol{H}_{\mathrm{ex}}$ is proportional to the magnetic moment of the Fe-sublattice $\boldsymbol{M}_{\mathrm{Fe}}$. The matrix elements of Eq.(1) are calculated by using the irreducible-tensor-operator technique. For a given applied field $\boldsymbol{H}$ and a direction of $\boldsymbol{H}_{\mathrm{ex}}$, the eigenvalues E_{i} and eigenfunctions $|n_i\rangle$ $[i = 1,2,\cdots,\sum_J(2J+1)]$ are obtained by diagonalizing the $\sum_J(2J+1)\times\sum_J(2J+1)$ matrix of Eq.(1). The diagonalization is carried out within the subspace of the ground J multiplet for the Tb and Ho ions and within the subspace of the ground and the two lowest excited J multiplets for the Sm ion with λ=410K.[19] The free energy for $R\mathrm{Fe}_{11}\mathrm{TiH}_x$ (x=0, 1) is given by

$$F(\boldsymbol{H},\boldsymbol{M}_{\mathrm{Fe}},T) = -kT\ln Z + K_1(T)\sin^2\theta_{\mathrm{Fe}} - \boldsymbol{M}_{\mathrm{Fe}}(T)\bullet\boldsymbol{H}, \quad (4)$$

where

$$Z = \sum_i \exp(-E_i/kT), \quad (5)$$

and $K_1(T)$ is the MCA constant of the Fe sublattice. $M_{\mathrm{Fe}}(T/T_{\mathrm{C}})/M_{\mathrm{Fe}}(0)$ and $K_1(T/T_{\mathrm{C}})/K_1(0)$ for $R\mathrm{Fe}_{11}\mathrm{Ti}$ and $R\mathrm{Fe}_{11}\mathrm{TiH}$ are considered to be the same as those for $\mathrm{LuFe}_{11}\mathrm{Ti}$ and $\mathrm{LuFe}_{11}\mathrm{TiH}$, respectively.[4] The values of $M_{\mathrm{Fe}}(0)$ for $R\mathrm{Fe}_{11}\mathrm{Ti}$ and $R\mathrm{Fe}_{11}\mathrm{TiH}$, which were adjusted around the values of $\mathrm{LuFe}_{11}\mathrm{Ti}$ and $\mathrm{LuFe}_{11}\mathrm{TiH}$ [2] respectively for better fit, are taken as 20.1 and 20.6 μ_{B}/f.u., respectively. For $\mathrm{HoFe}_{11}\mathrm{TiH}$ at 300K, the value of $M_{\mathrm{Fe}}(0)$=21.9μ_{B}/f.u. gives rise to a better fit. The values of $K_1(0)$ for $R\mathrm{Fe}_{11}\mathrm{Ti}$ and $R\mathrm{Fe}_{11}\mathrm{TiH}$ are taken as 23.6 and 26.6K/f.u., respectively, which are those for $\mathrm{LuFe}_{11}\mathrm{Ti}$ and $\mathrm{LuFe}_{11}\mathrm{TiH}$.[4] The equilibrium direction of $\boldsymbol{M}_{\mathrm{Fe}}$ is determined from minimization of $F(\boldsymbol{H},\boldsymbol{M}_{\mathrm{Fe}},T)$, and the magnetic moments of both the rare-earth ion and $R\mathrm{Fe}_{11}\mathrm{TiH}_x$ (x=0, 1) are given by

$$\boldsymbol{M}_R = -\mu_{\mathrm{B}}\sum_i < n_i\,|\boldsymbol{L}+2\boldsymbol{S}|\,n_i > \exp(-E_i/kT)/Z, \quad (6)$$

$$\boldsymbol{M} = \boldsymbol{M}_R + \boldsymbol{M}_{\mathrm{Fe}}. \quad (7)$$

For a magnetically aligned powder sample, it is assumed that the grains are non-interacting single domains in the fields above 1T and make the Gaussian distribution around the aligned direction (AD). The magnetizations along the direction parallel (z-axis) and perpendicular (x-axis) to the AD are, respectively,[16,17]

$$M_{//} = \frac{\int_{\theta_{\mathrm{c}}=0}^{\pi/2}\int_{\delta_{\mathrm{c}}=0}^{\pi/2} M_a\sin\theta_{\mathrm{c}}(-\sin\theta\sin\theta_{\mathrm{c}}\cos(\varphi+\delta_{\mathrm{c}})+\cos\theta\cos\theta_{\mathrm{c}})\exp\left(-\frac{\theta_{\mathrm{c}}^2}{2\theta_0^2}\right)\mathrm{d}\theta_{\mathrm{c}}\mathrm{d}\delta_{\mathrm{c}}}{\int_{\theta_{\mathrm{c}}=0}^{\pi/2}\int_{\delta_{\mathrm{c}}=0}^{\pi/2}\sin\theta_{\mathrm{c}}\exp\left(-\frac{\theta_{\mathrm{c}}^2}{2\theta_0^2}\right)\mathrm{d}\theta_{\mathrm{c}}\mathrm{d}\delta_{\mathrm{c}}}, \quad (8)$$

$$M_{\perp} = \frac{\int_{\theta_{\mathrm{c}}=0}^{\pi/2}\int_{\varphi_{\mathrm{c}}=0}^{\pi}\int_{\delta_{\mathrm{c}}=0}^{\pi/2} M_a\sin\theta_{\mathrm{c}}(\sin\theta\cdot p(\theta_{\mathrm{c}},\varphi_{\mathrm{c}},\delta_{\mathrm{c}},\varphi)+\cos\theta\sin\theta_{\mathrm{c}}\cos\varphi_{\mathrm{c}})\exp\left(-\frac{\theta_{\mathrm{c}}^2}{2\theta_0^2}\right)\mathrm{d}\theta_{\mathrm{c}}\mathrm{d}\varphi_{\mathrm{c}}\mathrm{d}\delta_{\mathrm{c}}}{\int_{\theta_{\mathrm{c}}=0}^{\pi/2}\int_{\varphi_{\mathrm{c}}=0}^{\pi}\int_{\delta_{\mathrm{c}}=0}^{\pi/2}\sin\theta_{\mathrm{c}}\exp\left(-\frac{\theta_{\mathrm{c}}^2}{2\theta_0^2}\right)\mathrm{d}\theta_{\mathrm{c}}\mathrm{d}\varphi_{\mathrm{c}}\mathrm{d}\delta_{\mathrm{c}}}, \quad (9)$$

$$p(\theta_{\mathrm{c}},\varphi_{\mathrm{c}},\delta_{\mathrm{c}},\varphi) = \cos\theta_{\mathrm{c}}\cos\varphi_{\mathrm{c}}\cos(\varphi+\delta_{\mathrm{c}}) - \sin\varphi_{\mathrm{c}}\sin(\delta_{\mathrm{c}}+\varphi). \quad (10)$$

Here, M_a is the absolute value of magnetization $\boldsymbol{M}$, θ_c and φ_c are the polar angles of the c-axis (z'-axis) in the xyz coordinate, and δ_c the angle between [100] (x'-axis) and the intersection line of the zoz' and the (001) ($x'oy'$) planes (Fig.1); θ and φ are the polar angles of the magnetization $\boldsymbol{M}$ in the $x'y'z'$ coordinate, and θ_0 is the alignment factor of the grains. The value of θ_0 can be determined from the remnant ratio of $M_{//}/M_{\perp}$.[20] By adding the projections of $\boldsymbol{M}$ of all the grains, $M_{//}$ and $M_{\perp}$ are calculated by using Eqs.(8) and (9).

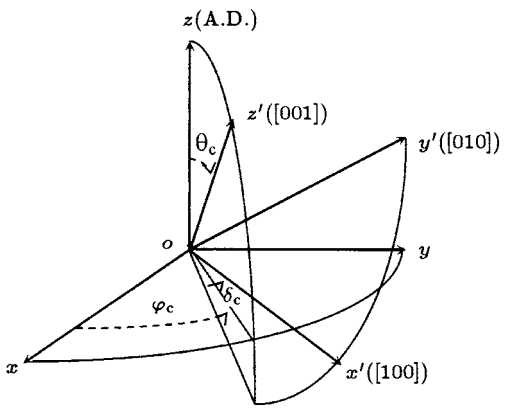


Fig.1. The xyz and $x'y'z'$ coordinate systems.

The values of the R–Fe exchange interaction $2\mu_B H_{ex}$ in RFe$_{11}$Ti and RFe$_{11}$TiH (R=Sm, Tb, Ho) are estimated as follows. The values of $2\mu_B H_{ex}$ (20K) derived by the INS experiment are about 470, 343 and 250 K for SmFe$_{11}$Ti [13], GdFe$_{11}$Ti[12] and ErFe$_{11}$Ti,[12] respectively. It is known that $2\mu_B H_{ex}$ decreases monotonically across the rare-earth series from Pr to Er in many Rare-earth-Fe intermetallic compounds.[21,22] By extrapolating the values of $2\mu_B H_{ex}$ (20K) for SmFe$_{11}$Ti, GdFe$_{11}$Ti and ErFe$_{11}$Ti to TbFe$_{11}$Ti and HoFe$_{11}$Ti, the values for the Tb and Ho compounds are estimated to be about 285 and 260K, respectively. The INS experiments on RFe$_{11}$Ti and RFe$_{11}$TiN (R=Gd, Er) show that the insertion of N into RFe$_{11}$Ti decreases $2\mu_B H_{ex}$ by ~14%.[12] The experiments on Gd$_2$Fe$_{17}$, Gd$_2$Fe$_{17}$N$_3$ and Gd$_2$Fe$_{17}$D$_3$ show that the deceases in $2\mu_B H_{ex}$ induced by the insertion of N and D are ~6 % and ~30 %, respectively.[18] It is assumed that the decrease induced by the insertion of H into RFe$_{11}$Ti is also one fifth of that induced by the insertion of N as for the 2:17 compound. In this way the values of $2\mu_B H_{ex}$ (20K) for SmFe$_{11}$TiH, TbFe$_{11}$TiH and HoFe$_{11}$TiH are estimated to be about 457, 277 and 253K, respectively.

The values of CEF parameters A_{nm} are evaluated by fitting the calculations to the magnetization curves measured on the SmFe$_{11}$Ti and RFe$_{11}$TiH$_x$ (R=Tb, Ho) (x=0, 1) single crystals and on the magnetically aligned SmFe$_{11}$TiH at different temperatures.

3. Results and discussions

Table 1 lists the fitted values of CEF parameters A_{nm} for RFe$_{11}$Ti and RFe$_{11}$TiH (R=Sm, Tb, Ho). It can be seen that the insertion of H does not change the negative sign of A_{20} but increases the absolute values markedly. In this connection, the Mössbauer study of ^{155}Gd in GdFe$_{11}$TiH$_x$ (x=0, 1) has shown that the hydrogenation leads to an about 53% increase of the electric field gradient at Gd ion site.[8] The gradient is proportional to A_{20}. The values of high-order CEF parameters for RFe$_{11}$TiH are quite different from those for RFe$_{11}$Ti. The change of magnetic anisotropy induced by the insertion of H originates mainly from the change of CEF parameters. For example, the change of the easy magnetization direction from [100] to [110] for TbFe$_{11}$Ti is caused by the change of the sign of A_{44}.

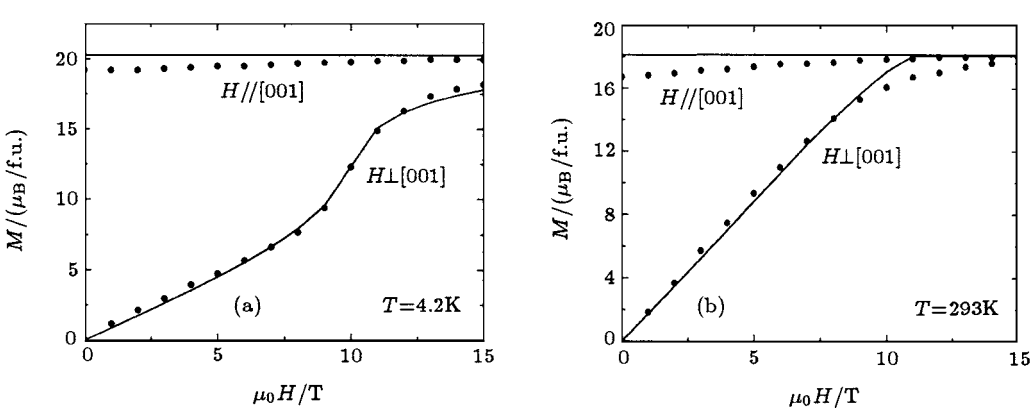


Fig.2. Magnetization curves of SmFe$_{11}$Ti at 4.2 (a) and 293K (b): •••, experimental data from Ref.[13]; —, the calculation.

Table 1. The fitted values of CEF parameters A_{nm} (all in units of K).

	A_{20}	A_{40}	A_{44}	A_{60}	A_{64}
$SmFe_{11}Ti$	–240	20	–	880	–
$SmFe_{11}TiH$	–320	130	–	750	–
$TbFe_{11}Ti$	–90	–4	–125	2	–87
$TbFe_{11}TiH$	–172	–110	30	25	–31
$HoFe_{11}Ti$	–61	–122	–176	432	–13
$HoFe_{11}TiH$	–132	–89	–68	87	2

The uncertainty of each parameter can be seen from the following data on $SmFe_{11}Ti$ and $TbFe_{11}Ti$ at 4.2K, which demonstrates the variation in the calculation of the most sensitively affected quantity when the value of each parameter is changed separately. An increase in $|A_{20}|$ by 8% or in $|A_{40}|$ by 50% or in $|A_{60}|$ by 35% changes the $M(\mu_0 H = 9\text{T})$ along the basal plane for $SmFe_{11}Ti$ from 9.54 to 8.78 or 9.72 or 8.52μ_B/f.u. respectively. An increase in $|A_{44}|$ by 24% or in $|A_{64}|$ by 34% changes the M ($\mu_0 H = 8\text{T}$) along the [001] axis for $TbFe_{11}Ti$ from 9.66 to 8.68 or 10.15μ_B/f.u..

Figures 2 to 8 show the comparisons of the calculations with the experimental data. The symbols represent experimental data and curves and calculations. The calculations reproduce the experimental data well. Figures 2(a) and (b) show the magnetization curves along the [001] axis and the basal plane at 4.2 and 293K for the $SmFe_{11}Ti$ single crystal. Figure 3 shows the magnetization curve along the direction perpendicular to the AD at 4.2K for the aligned $SmFe_{11}Ti$. The parameters used in the calculation for the aligned $SmFe_{11}Ti$ are those obtained from the fit of the calculations to the experimental data for the

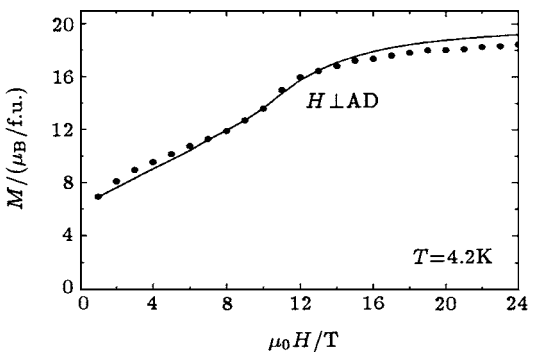


Fig.3. Magnetization curve at 4.2K for aligned $SmFe_{11}Ti$: • • •, experimental data from Ref.[6]; —, the calculation (θ_0=24°).

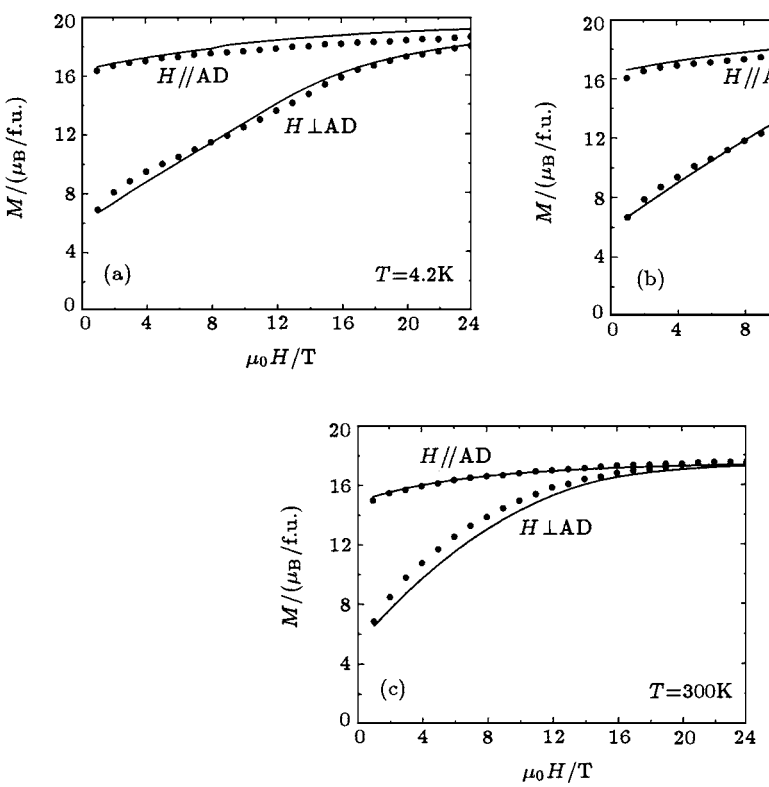


Fig.4. Magnetization curves at 4.2 (a), 120 (b) and 300K (c) for aligned $SmFe_{11}TiH$: • • •, experimental data from Ref.[6] and Ref.[7]; —, the calculation (θ_0=24°).

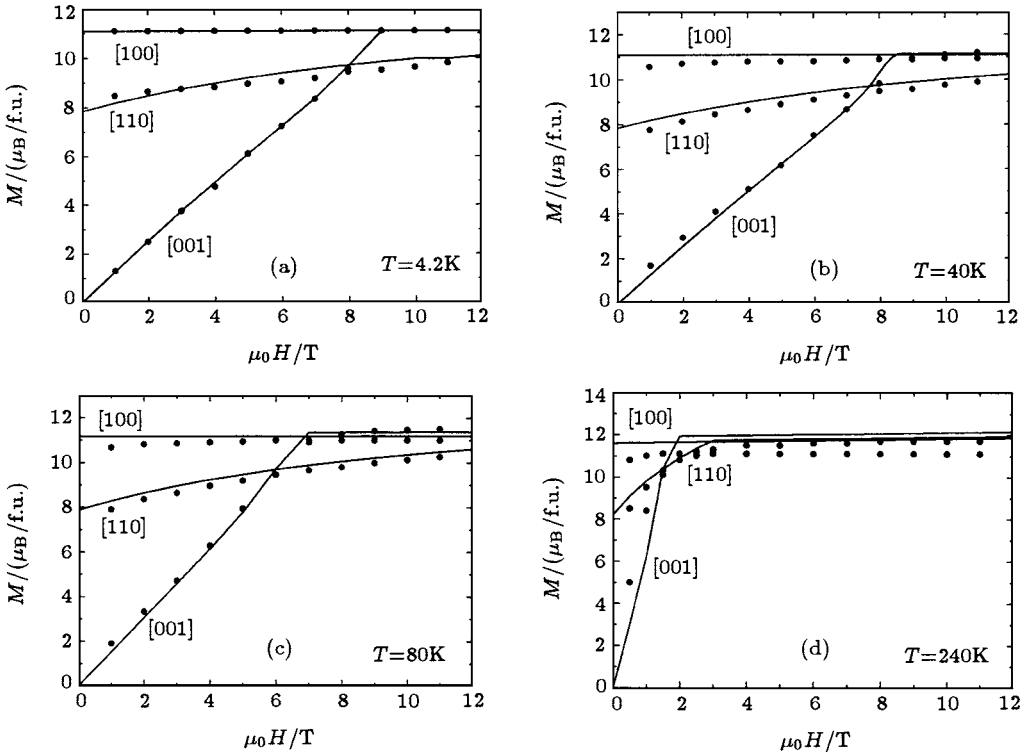


Fig.5. Magnetization curves of $TbFe_{11}Ti$ at 4.2 (a), 40 (b), 80 (c) and 240K (d): •••, experimental data from Ref.[2] and Ref.[9]; —, the calculation.

$SmFe_{11}Ti$ single crystal. Figures 4(a), (b) and (c) show the magnetization curves along the directions parallel and perpendicular to the AD at 4.2, 120 and 300K for the aligned $SmFe_{11}TiH$. Figures 5(a), (b), (c) and (d) show the magnetization curves along the [100], [110] and [001] axes at 4.2, 40, 80 and 240K for the $TbFe_{11}Ti$ single crystal respectively. Figure 6 shows the magnetization curves along the [100], [110] and [001] axes at 4.2K for the $TbFe_{11}TiH$ single crystal. Figures 7(a) and (b) show the magnetization curves along the [100], [110] and [001] axes respectively at 4.2 and 290K for the $HoFe_{11}Ti$ single crystal. Figures 8(a) and (b) show the magnetization curves along the [100], [110] and [001] axes respectively at 4.2 and 300K for the $HoFe_{11}TiH$ single crystal. In Fig.8(b), the solid curves represent the calculations with $M_{Fe}(0)=20.6\mu_B$/f.u. and the dashed curves with $M_{Fe}(0)=21.9\mu_B$/f.u..

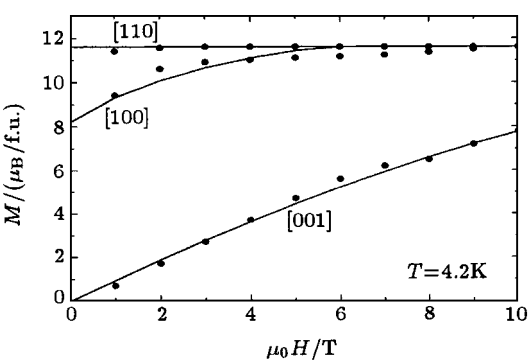


Fig.6. Magnetization curves of $TbFe_{11}TiH$ at 4.2K: •••, experimental data from Ref.[2]; —, the calculation.

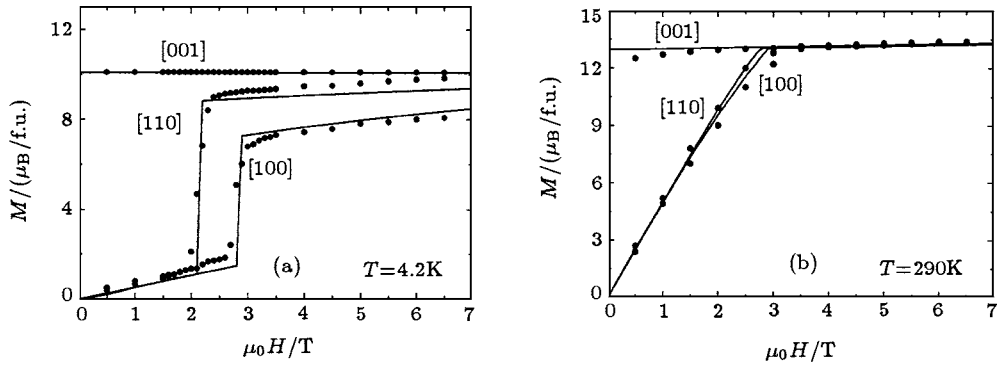


Fig.7. Magnetization curves of $HoFe_{11}Ti$ at 4.2 (a) and 290K (b): • • •, experimental data from Ref.[1] and Ref.[9]; —, the calculation.

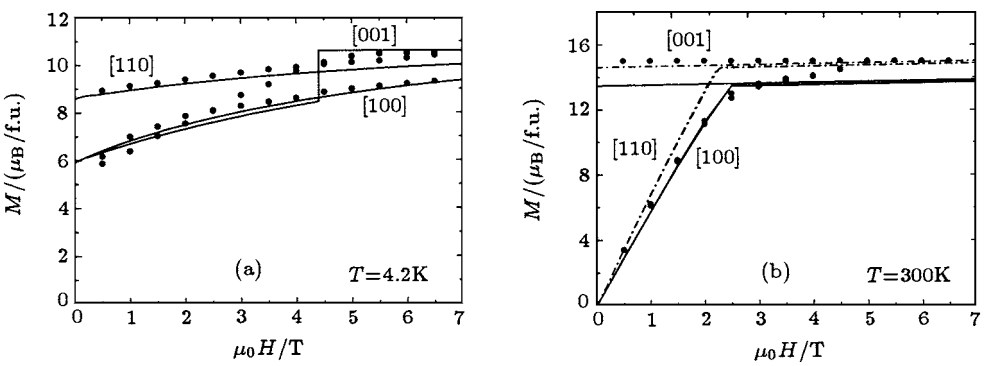


Fig.8. Magnetization curves of $HoFe_{11}TiH$ at 4.2 (a) and 300K (b): • • •, experimental data from Ref.[1] and Ref.[10]; —, the calculation ($M_{Fe}(0)=20.6\mu_B$/f.u.); —, the calculation ($M_{Fe}(0)=21.9\mu_B$/f.u.).

References

[1] Nikitin S A, Tereshina I S, Pankratov N Yu and Skourski Yu V 2001 *Phys. Rev.* B **63** 134420

[2] Nikitin S A, Tereshina I S, Verbetsky V N, Salamova A A, Skokov K P, Pankratov N Yu, Skourski Yu V, Tristan N V, Zubenko V V and Telegina I V 2001 *J. Alloys Comp.* **322** 42

[3] Tereshina I S, Gaczynski P, Rusakov V S, Drulis H, Nikitin S A, Suski W, Tristan N V and Palewski T 2000 *J. Phys.: Condens. Matter* **13** 8161

[4] Tereshina I S, Nikitin S A, Pankratov N Yu, Bezkorovajnaya G A, Salamova A A, Verbetsky V N, Mydlarz T and Skourski Yu V 2001 *J. Magn. Magn. Mater.* **231** 213

[5] Nikitin S A, Tereshina I S, Verbetsky V N and Salamova A A 2001 *J. Alloys Comp.* **316** 46

[6] Isnard O, Guillot M, Miraglia S and Fruchart D 1996 *J. Appl. Phys.* **79** 5542

[7] Isnard O, Miraglia S, Guillot M and Fruchart D 1998 *J. Alloys Comp.* **275/277** 637

[8] Isnard O, Vulliet P, Sanchez J P and Fruchart D 1998 *J. Magn. Magn. Mater.* **189** 47

[9] Abadia C, Algarabel P A, Garcia-Landa B, Moral A del, Kudrevatykh N V and Markin P E 1998 *J. Phys.: Condens. Matter* **10** 349

[10] Nikitin S A, Tereshina I S, Skourski Yu V, Pankratov N Yu, Skokov K P, Zubenko V V and Telegina I V 2001 *Physics of the Solid State* **43** 290

[11] Piquer C, Isnard O, Grandjean F and Long G J 2003 *J. Magn. Magn. Mater.* **265** 156

[12] Hurley D P F, Kuz'min M, Coey J M D and Kohgi M 1995 *J. Magn. Magn. Mater.* **140/144** 1027

[13] Moze O, Caciuffo R, Li H S, Hu B P, Coey J M D, Osborn R and Taylor A D 1990 *Phys. Rev.* B **42** 1940

[14] Hu B P, Li H S, Coey J M D and Gavigan J P 1990 *Phys. Rev.* B **41** 2221

[15] Yan Y, Xu S W, Jin H M, Du X B and Su F 2004 *Chin. Phys.* **13** 1965

[16] Yan Y, Jin H M and Kim Y B 2000 *J. Magn. Magn. Mater.* **221** 382

[17] Yan Y and Jin H M 2000 *Acta Phys. Sin.* **49** 1362 (in Chinese)

[18] Isnard O, Sippel A, Loewenhaupt M and Bewley R 2001 *J. Phys.: Condens. Matter* **13** 3533

[19] Hufner S 1978 *Optical Spectra of Transparent Rare-earth Compounds* (London: Academic) p34

[20] Kim Y B and Jin H M 1997 *J. Magn. Magn. Mater.* **169** 114

[21] Belorizky E, Fremy M A, Gavigan J P, Givord D and Li H S 1987 *J. Appl. Phys.* **61** 3971

[22] Loewenhaupt M and Sosnowska I 1991 *J. Appl. Phys.* **70** 5967